EC Journals.ASM.org

Trypanosoma brucei Bloodstream Forms Depend upon Uptake of *myo*-Inositol for Golgi Complex Phosphatidylinositol Synthesis and Normal Cell Growth

Amaia González-Salgado,[a] Michael Steinmann,[a] Louise L. Major,[b] Erwin Sigel,[a] Jean-Louis Reymond,[c] Terry K. Smith,[b] Peter Bütikofer[a]

Institute of Biochemistry and Molecular Medicine, University of Bern, Bern, Switzerland[a]; Biomedical Sciences Research Complex, University of St Andrews, North Haugh, St. Andrews, Fife, United Kingdom[b]; Department of Chemistry and Biochemistry, University of Bern, Bern, Switzerland[c]

***myo*-Inositol is a building block for all inositol-containing phospholipids in eukaryotes. It can be synthesized *de novo* from glucose-6-phosphate in the cytosol and endoplasmic reticulum. Alternatively, it can be taken up from the environment via Na^+- or H^+-linked *myo*-inositol transporters. While Na^+-coupled *myo*-inositol transporters are found exclusively in the plasma membrane, H^+-linked *myo*-inositol transporters are detected in intracellular organelles. In *Trypanosoma brucei*, the causative agent of human African sleeping sickness, *myo*-inositol metabolism is compartmentalized. *De novo*-synthesized *myo*-inositol is used for glycosylphosphatidylinositol production in the endoplasmic reticulum, whereas the *myo*-inositol taken up from the environment is used for bulk phosphatidylinositol synthesis in the Golgi complex. We now provide evidence that the Golgi complex-localized *T. brucei* H^+-linked *myo*-inositol transporter (TbHMIT) is essential in bloodstream-form *T. brucei*. Downregulation of TbHMIT expression by RNA interference blocked phosphatidylinositol production and inhibited growth of parasites in culture. Characterization of the transporter in a heterologous expression system demonstrated a remarkable selectivity of TbHMIT for *myo*-inositol. It tolerates only a single modification on the inositol ring, such as the removal of a hydroxyl group or the inversion of stereochemistry at a single hydroxyl group relative to *myo*-inositol.**

In all eukaryotes, *myo*-inositol is the precursor for all inositol-containing phospholipids, including phosphatidylinositol (PI), phosphatidylinositol (poly)phosphates, inositol phosphorylceramide (IPC), and glycosylphosphatidylinositol (GPI). In mammalian cells, it is taken up from the environment via sodium/*myo*-inositol cotransporters (SMITs) or proton-linked *myo*-inositol transport (*T. brucei* H^+-linked *myo*-inositol transporter [TbHMIT]). Human SMIT1 and SMIT2 belong to the sodium/glucose transporter family, SGLT/SLC5, whose members in general mediate uptake of sugars and osmolytes in the gastrointestinal tract and the kidney (1). They are localized in the plasma membrane and, besides *myo*-inositol, also transport xylose and glucose (2, 3). In contrast, the human HMIT belongs to the sugar/polyol transport facilitator family, GLUT/SLC2A (4). While most members of this family are also located in the plasma membrane and regulate sugar homeostasis within the body, members of the family of subclass III transporters, to which HMIT belongs, are typically localized intracellularly (5, 6). Interestingly, GLUT12/SLC2A12 and HMIT/SLC2A13 have been found to colocalize with Golgi complex markers (7, 8). Although the substrate specificities of the subclass III GLUT/SLC2A transporters have been studied in model systems, their physiological roles have not been firmly established (5, 6). Notably, HMIT completely lacks sugar transport activity but instead transports *myo*-inositol with a K_m of approximately 100 μM in a *Xenopus* oocyte expression system (8).

As an alternative to uptake, *myo*-inositol can be synthesized *de novo* in a reaction sequence that is conserved from bacteria to mammals, using glucose-6-phosphate as an initial substrate (9). Endogenously produced as well as imported *myo*-inositol can then be used for inositol phospholipid synthesis in a process that is generally believed to occur in the endoplasmic reticulum (ER). In yeast, plants, protozoa, and mammals, PI synthase has been localized to the ER using cell fractionation and immunolocalization studies (10–13). Reconstitution experiments involving purified PI synthase from *Saccharomyces cerevisiae* showed that it incorporates asymmetrically into model vesicles, suggesting that its active site may face the cytosolic side of the ER in yeast (10). However, the *in vivo* topology of the active site of PI synthase has not been determined experimentally.

Interestingly, recent reports in protozoan parasites indicated that the Golgi complex represents an additional site for inositol phospholipid synthesis. Direct evidence for the presence of PI synthase in the Golgi complex was obtained from immunolocalization studies in *Trypanosoma brucei* bloodstream forms (13), showing that the enzyme has a dual localization in the ER and Golgi complex. In support of the idea of the Golgi complex being the site of bulk PI synthesis in trypanosomes (13), a subsequent study revealed that *T. brucei* procyclic forms express a plasma membrane- and Golgi complex-localized proton-linked *myo*-inositol transporter, TbHMIT (14). Downregulation of TbHMIT in-

Received 3 March 2015 **Accepted** 13 April 2015

Accepted manuscript posted online 17 April 2015

Citation González-Salgado A, Steinmann M, Major LL, Sigel E, Reymond J-L, Smith TK, Bütikofer P. 2015. *Trypanosoma brucei* bloodstream forms depend upon uptake of *myo*-inositol for Golgi complex phosphatidylinositol synthesis and normal cell growth. Eukaryot Cell 14:616–624. doi:10.1128/EC.00038-15.

Address correspondence to Terry K. Smith, tks1@st-andrews.ac.uk, or Peter Bütikofer, peter.buetikofer@ibmm.unibe.ch.

Supplemental material for this article may be found at http://dx.doi.org/10.1128/EC.00038-15.

doi:10.1128/EC.00038-15

hibited bulk PI formation but had no effect on GPI synthesis, demonstrating that PI synthesis in *T. brucei* is compartmentalized, with the Golgi complex representing the site of synthesis of bulk membrane PI utilizing exogenous *myo*-inositol (14) and the ER being the site of PI synthesis for GPI production utilizing *de novo*-synthesized *myo*-inositol (15). Transporter-mediated *myo*-inositol uptake has also been characterized in other protozoan parasites, including *Leishmania donovani* (16–19) and *Trypanosoma cruzi* (20, 21). These parasites all cause devastating human diseases, including leishmaniasis, Chagas disease, and human African sleeping sickness. Membrane transporters are of particular importance for these pathogens to acquire essential nutrients from their respective hosts and offer attractive targets for rational drug design and/or the delivery of cytotoxic substrate analogues. The reported dependence of *T. brucei* procyclic forms in culture on the presence of exogenous *myo*-inositol (13, 14) validates HMIT as a potential drug target.

In this report, we extend our previous analysis of *myo*-inositol uptake in *T. brucei* procyclic forms to the pharmacologically more relevant bloodstream form. We demonstrate that expression of TbHMIT is essential for normal growth of *T. brucei* bloodstream parasites in culture and that it is involved in *myo*-inositol transport and PI formation within the Golgi complex. In addition, we have tested a series of *myo*-inositol stereoisomers and structural analogs and related compounds to characterize the substrate specificity of TbHMIT.

MATERIALS AND METHODS

Unless otherwise stated, all reagents were of analytical grade and purchased from Merck (Darmstadt, Germany), Sigma-Aldrich (Buchs, Switzerland), or ICN Biomedicals (Tägerig, Switzerland). Antibiotics and fetal bovine serum (FBS) were obtained from Invitrogen (Basel, Switzerland). Primers and sequencing services were from Microsynth AG (Balgach, Switzerland). Restriction enzymes were purchased from Thermo Scientific (Wohlen, Switzerland). *myo*-[2-^{3}H(N)]inositol (15 to 20 Ci/mmol) (*myo*-[^{3}H]inositol) and [^{3}H]ethanolamine (40 to 60 Ci/mmol) were from American Radiolabeled Chemicals (St. Louis, MO, USA), and dCTP-[α-^{32}P] (3000 Ci/mmol) was from PerkinElmer Life Sciences (Schwerzenbach, Switzerland).

Trypanosomes and culture conditions. Bloodstream-form *T. brucei* parasites derived from line MiTat 1.2, coexpressing T7 RNA polymerase and a tetracycline repressor (22), were cultured at 37°C with 5% CO_2 in HMI-9 (23) containing 10% heat-inactivated FBS and 1 μg/ml G418. *T. brucei* strain 427 procyclic forms were cultured at 27°C in SDM-79 (24) containing 5% heat-inactivated FBS.

RNAi-mediated gene silencing. Expression of TbHMIT (Tb927.11.5350) was downregulated in *T. brucei* bloodstream forms by RNA interference (RNAi)-mediated gene silencing using a stem-loop construct containing a phleomycin resistance gene. The stem-loop was excised from plasmid pAG3020 (14) using BamHI and HindIII and religated into plasmid pMS1720RNAiBSF (25), resulting in plasmid pAG3020-BSF. Plasmid extraction was performed using a Qiagen Plasmid Midi kit (Qiagen, Hilden, Germany) according to the manufacturer's instructions. Before transfection of *T. brucei* bloodstream forms, plasmid DNA was linearized with NotI and precipitated with phenol and chloroform.

Generation of HA-tagged TbHMIT. Overexpression of C-terminal 3× hemagglutinin (HA)-tagged TbHMIT was performed using inducible vector pALC14 as described previously (14), resulting in plasmid pAG3020-BSF2. Before transfection of *T. brucei* bloodstream forms, plasmid DNA was linearized with NotI and isolated with phenol and chloroform.

Stable transfection of trypanosomes and selection of clones. *T. brucei* bloodstream forms (4×10^7 to 5×10^7 cells) were harvested at mid-log phase (0.8×10^6 to 1.1×10^6 cells/ml) by centrifugation at 1,250 × *g* for 10 min, suspended in 100 μl of buffer (26) (90 mM $NaPO_4$, 5 mM KCl, 0.15 mM $CaCl_2$, 50 mM HEPES, pH 7.3), and mixed with 10 μg of linearized plasmid pAG3020-BSF or pAG3020-BSF2. Electroporation was performed in a 0.2-cm-gap pulse cuvette (Bio-Rad Laboratories, Reinach, Switzerland) with a Lonza Nucleofector system (Ruwag Lifescience, Bettlach, Switzerland) using program FI-115. Electroporated cells were immediately inoculated in 10 ml of HMI-9, containing 10% heat-inactivated FBS, and, if required for selection, 1 μg/ml phleomycin (for RNAi) or 0.1 μg/ml puromycin (for overexpression). Clones were obtained by limiting dilutions in 24-well plates in HMI-9, containing 10% heat-inactivated FBS, in the presence of 1 μg/ml phleomycin or 0.1 μg/ml puromycin. Antibiotic-resistant clones were tested for the presence of the introduced gene by PCR. Expression of HA-tagged TbHMIT or induction of RNAi was started by addition of 1 μg/ml tetracycline to parasite cultures.

RNA isolation and Northern blot analysis. Total RNA for Northern blotting was isolated using a Total SV RNA extraction kit (Promega, Dübendorf, Switzerland), following the manufacturer's instructions. RNA (10 μg) was separated on formaldehyde-agarose gels (1% agarose–2% formaldehyde–3-N-morpholino propane sulfonic acid) and transferred to GeneScreen Plus nylon membranes (PerkinElmer Life Sciences). ^{32}P-labeled probes were made by random priming of the same PCR products as were used as insertions in the stem-loop vector using a Prime-a-Gene labeling system (Promega). Hybridization was performed overnight at 60°C in hybridization buffer containing 7% (wt/vol) SDS, 1% (wt/vol) bovine serum albumin, 0.9 mM EDTA, and 0.5 M Na_2HPO_4 (pH 7.2), and the membrane was analyzed by autoradiography using BioMax mass spectrometry (MS) film and a TransScreen-HE intensifying screen. rRNA was visualized on the same formaldehyde-agarose gel by ethidium bromide staining to control for equal loading.

***myo*-Inositol uptake assays.** *T. brucei* bloodstream forms (1×10^8 cells) at the mid-log phase were harvested by centrifugation at 1,250 × *g* for 10 min and suspended in phosphate-buffered saline (PBS; 135 mM NaCl, 1.3 mM KCl, 3.2 mM Na_2HPO_4, 0.5 mM KH_2PO_4, pH 7.4) at 27°C. Uptake of *myo*-[^{3}H]inositol was measured by adding 50 nM *myo*-[^{3}H]inositol to cells at 37°C. At various time points, uptake of the label was terminated by pelleting 1.5×10^7 parasites by centrifugation (1,500 × *g*, 5 min, 4°C) and washing three times in ice-cold PBS. After resuspension of the pellet in 100 μl PBS, radioactivity was measured by scintillation counting using a Packard Tri-Carb 2100TR liquid scintillation analyzer (PerkinElmer Life Sciences). Aliquots of the parasite suspensions before centrifugation were used to determine the total amount of radioactivity in the assay.

Metabolic labeling of trypanosomes, lipid extraction, and TLC. Metabolic labeling of trypanosomes was performed as described before (27). Briefly, *myo*-[^{3}H]inositol was added to bloodstream-form or procyclic trypanosomes at mid-log phase, and incubation was continued for 16 h. Cells were harvested by centrifugation at 1,750 × *g* for 10 min and washed with ice-cold Tris-buffered saline (10 mM Tris, 144 mM NaCl, pH 7.4) to remove unincorporated label, and bulk phospholipids were extracted twice with 10 ml chloroform:methanol (CM; 2:1 [vol/vol]). CM fractions were pooled, dried under nitrogen, and resuspended in a small volume of CM. Aliquots were treated with 6 μl PI-specific phospholipase C from *Bacillus cereus* (Thermo Scientific, Wohlen, Switzerland) for 60 min, as described elsewhere (28). Lipids were analyzed by thin-layer chromatography (TLC) on Silica Gel 60 plates (Merck) using solvent system 1, composed of chloroform:methanol:acetic acid:water (25:15:4:2 [vol/vol/vol/vol]) (29). Appropriate lipid standards were run alongside the samples to be analyzed. Radioactivity was detected by scanning the air-dried plate with a radioisotope detector (Berthold Technologies, Regensdorf, Switzerland) and quantified using the Rita Star software provided by the manufacturer. For analysis of GPI precursors, bloodstream-form trypanosomes were labeled for 16 h with trace amounts of [^{3}H]ethanolamine (28). After the cells were harvested and bulk lipids were extracted as described above, GPI lipids were extracted from the pellet using chloroform:methanol:water (10:10:3 [vol/vol/vol]) and partitioned between water

and butan-1-ol. [^{3}H]-labeled GPI lipids in the butan-1-ol-rich upper phase were analyzed by TLC using solvent system 2, composed of chloroform:methanol:water (10:10:3 [vol/vol/vol]) (28). Radioactivity was detected as described above.

Mass spectrometry and inositol analysis. Total lipids for mass spectrometry analysis were extracted using a modification of the Bligh and Dyer method (30). Briefly, *T. brucei* bloodstream forms were collected at the mid-log phase, washed with PBS, resuspended in 100 μl of fresh PBS, and transferred to a glass tube. Chloroform:methanol (1:2 [vol/vol]) (375 ml) was then added and subjected to vigorous vortex mixing for 10 to 15 min. The sample was made biphasic by the addition of 125 ml chloroform and 125 ml water, subjected to vortex mixing again, and centrifuged at 1,000 × *g* at room temperature (RT) for 5 min. The lower phase was dried under nitrogen and stored at 4°C. Total lipid extracts were dissolved in 15 ml of choloroform:methanol (1:2 [vol/vol])–15 ml of acetonitrile:*iso*-propanol:water (6:7:2 [vol/vol/vol]) and analyzed with a Absceix 4000 QTrap, a triple-quadrupole mass spectrometer equipped with a nanoelectrospray source. Samples were delivered using a Nanomate interface in direct infusion mode (~125 nl/min). Lipid extracts were analyzed in both positive- and negative-ion modes using a capillary voltage of 1.25 kV. Tandem mass spectrometry (MS/MS) scanning (daughter, precursor, and neutral loss scans) was performed using nitrogen as the collision gas with collision energies of between 35 and 90 V. Each spectrum encompassed at least 50 repetitive scans. MS/MS spectra were obtained with collision energies as follows: 35 to 45 V, phosphatidylcholine-sphingomyelin (PC/SM) in positive-ion mode, parent-ion scanning of *m/z* 184; 35 to 55 V, PI in negative-ion mode, parent-ion scanning of *m/z* 241; 35 to 65 V, phosphatidylethanolamine (PE) in negative-ion mode, parent-ion scanning of *m/z* 196; 20 to 35 V, phosphatidylserine (PS) in negative-ion mode, neutral loss scanning of *m/z* 87; and 40 to 90 V. MS/MS daughter ion scanning was performed with collision energies of between 35 and 90 V. Assignment of phospholipid species is based upon a combination of survey, daughter, precursor and neutral loss scans, as well previous assignments (31). The identity of phospholipid peaks was verified using the LIPID Metabolites And Pathways Strategy (LIPID MAPS) Nature Lipidomics Gateway (www.lipidmaps.org).

For the inositol analysis, bloodstream forms were collected and lipids were extracted as described above. An internal standard of D_6 *myo*-inositol was added to samples prior to hydrolysis by strong acid (6 M HCl, 110°C), derivatization with tetramethylsilane (TMS), and analysis by gas chromatography-mass spectrometry, as published elsewhere (32). *myo*-Inositol was quantified, and the means and standard deviations of the results of three separate analyses were determined.

Microscopy. For immunolocalization of HA-tagged TbHMIT, trypanosomes were cultured in the presence of tetracycline for 24 h to induce protein expression and processed as described previously (14). HA-tagged proteins were detected using monoclonal mouse anti-HA antibody (Covance, Munich, Germany) at a dilution of 1:250 in PBS for 1 h at room temperature. The Golgi complex was visualized by incubating fixed parasites for 1 h at room temperature with rabbit anti-TbGRASP antibody (kindly provided by G. Warren, University of Vienna) (used at a dilution of 1:1,000). Subsequently, the slides were washed three times with PBS and incubated with the corresponding secondary antibodies, Alexa Fluor 594 goat anti-mouse IgG and Alexa Fluor 488 goat anti-rabbit IgG (Invitrogen), at dilutions of 1:1,000 and 1:500, respectively, for 1 h at room temperature. Slides were washed three times with PBS and mounted using Vectashield containing 4′,6-diamidino-2-phenylindol (DAPI; Vector Laboratories, Burlingame, CA, USA). Fluorescence microscopy was performed on a Leica AF6000 microscope (Leica Microsystems, Heerbrugg, Switzerland), using the software provided by the manufacturer.

Substrate specificity of TbHMIT. *Xenopus laevis* oocytes were prepared, injected with Tb927.11.5350 cRNA, and defollicated as described previously (14). Electrophysiological experiments were performed as described before (14). *myo*-Inositol, *epi*-quercitol, *vibo*-quercitol, *proto*-quercitol, *scyllo*-inositol, *muco*-inositol, *allo*-inositol, *epi*-inositol, 1D-*chiro*-inositol, 1L-*chiro*-inositol, 1L-*epi*-2-inosose, phytic acid, L-quebrachitol, D-pinitol, N-00601 [(1R,4S)-6-methoxycyclohexane-1,2,3,4,5-pentol], N-50350 [(1R,3S)-6-methoxycyclohexane-1,2,3,4,5-pentol], and D-*myo*-inositol-3-phosphate at 200 μM were applied for 20 s for each measurement. Potential inhibition of TbHMIT was tested by applying a combination of 200 μM *myo*-inositol and one of the compounds described above at equal concentrations. The resulting signal was compared with that elicited by 200 μM *myo*-inositol alone.

RESULTS AND DISCUSSION

Characterization of *T. brucei* TbHMIT in bloodstream-form parasites. To study whether TbHMIT is essential in *T. brucei* bloodstream forms in culture, we generated tetracycline-inducible RNAi cell lines against Tb927.11.5350. Transfection of *T. brucei* bloodstream forms with plasmid pAG3020-BSF and selection by resistance to phleomycin resulted in several clones, one of which (A3) was selected for all subsequent experiments. After 2 days of induction of RNAi by addition of tetracycline to the culture, parasite growth decreased compared to that seen with uninduced (control) cells (Fig. 1A). Northern blot analysis showed that after 2 days of RNAi treatment, Tb927.11.5350 mRNA was undetectable (Fig. 1A, inset). The uptake of *myo*-inositol into bloodstream-form RNAi parasites was measured by adding trace amounts of *myo*-[^{3}H]inositol to trypanosomes cultured for 2 days in the absence or presence of tetracycline and measuring radioactivity in the cell pellets after centrifugation. The results show that uptake of *myo*-[^{3}H]inositol into control trypanosomes increased linearly over 90 min (Fig. 1B). A similar time-dependent linear increase in cell-associated radioactivity was also observed for RNAi parasites after downregulation of TbHMIT; however, uptake of *myo*-[^{3}H]inositol was reduced to approximately half of that in control cells. To demonstrate that the *myo*-[^{3}H]inositol that was taken up was being metabolized into inositol-containing phospholipids, bloodstream forms cultured in the absence or presence of tetracycline were incubated for 16 h in the presence of *myo*-[^{3}H]inositol followed by analysis of radiolabeled lipids by TLC and radioactivity scanning. In the absence of tetracycline, a single [^{3}H]-labeled lipid class was detected (Fig. 1C, top panel; see also Fig. S1A in the supplemental material) and was identified as [^{3}H]PI based on its comigration with a commercial PI standard and complete susceptibility to PI-specific phospholipase C (see Fig. S1B). After RNAi-mediated downregulation of TbHMIT, formation of [^{3}H]PI in parasites was reduced by >85% (Fig. 1C, middle panel). No formation of [^{3}H]inositol phosphorylceramide ([^{3}H]IPC), which is readily labeled in procyclic forms (Fig. 1C, bottom panel; see also reference 14), was observed in uninduced bloodstream forms. This observation is consistent with previous reports showing that IPC synthesis is largely absent in *T. brucei* bloodstream forms (31, 33). In addition, we analyzed the formation of GPI precursor lipids by labeling bloodstream-form parasites cultured in the absence or presence of tetracycline with [^{3}H]ethanolamine, which gets incorporated into GPIs (28). As shown in Fig. 1D, formation of the major ^{3}H-labeled GPI precursors, P2 and P3, was readily observed in parasites after depletion of TbHMIT. This result demonstrates that, as previously shown in procyclic forms (14), GPI synthesis is not affected by downregulation of TbHMIT.

The effect of TbHMIT RNAi on parasite lipid composition was investigated by extracting the lipids and analyzing them by electrospray-MS (ES-MS). In negative-ion mode, a range of peaks was observed in the uninduced RNAi cells that corresponded to the

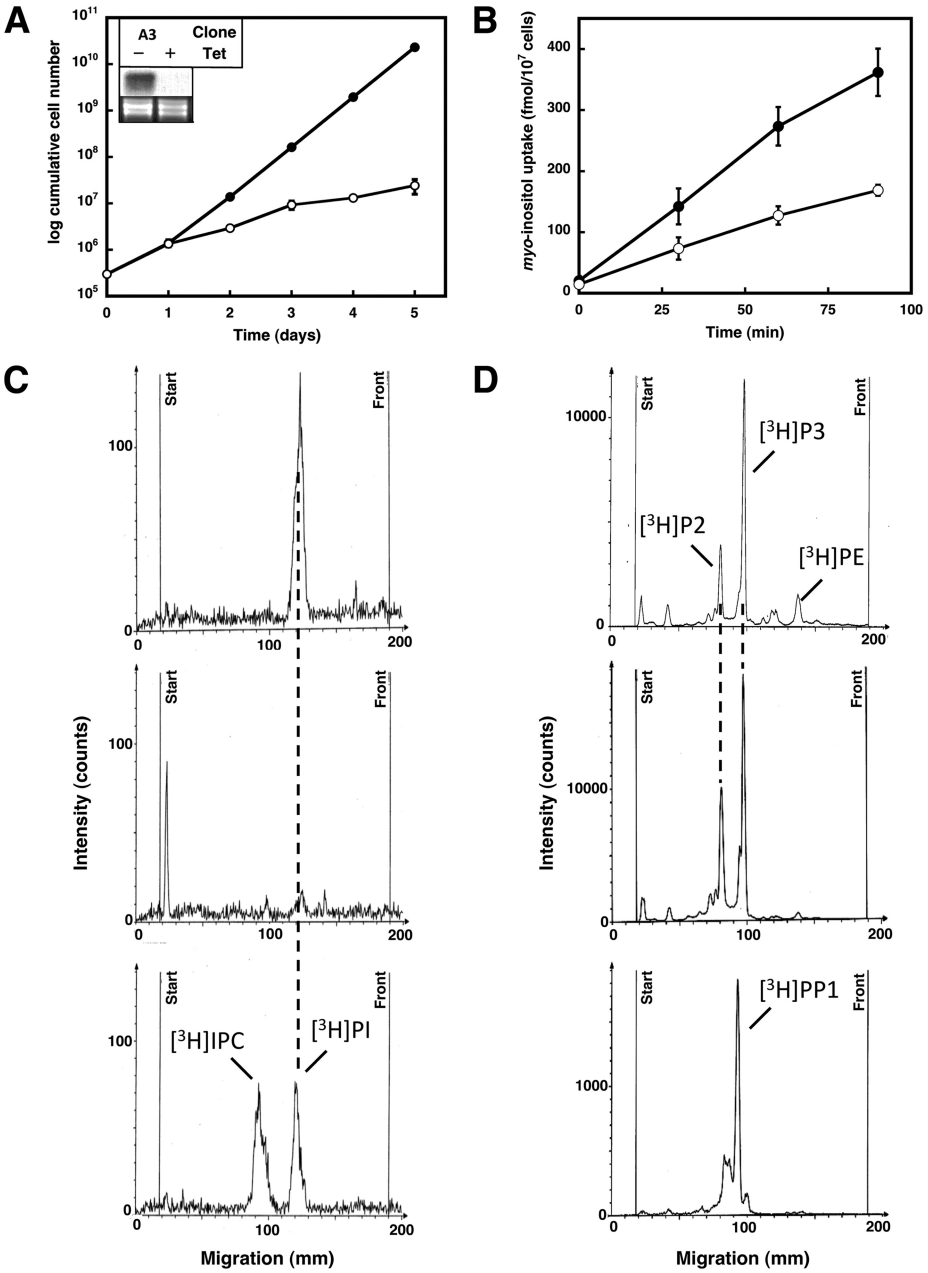

FIG 1 Essentiality of TbHMIT in *T. brucei* bloodstream forms. (A) Growth of *T. brucei* bloodstream-form RNAi parasites. Expression of TbHMIT in *T. brucei* bloodstream forms was downregulated by tetracycline (Tet)-inducible RNAi, and growth of trypanosomes was monitored for 5 days. Data points represent cumulative numbers of RNAi cells incubated in the absence (filled symbols) or presence (open symbols) of tetracycline and correspond to mean values ± standard deviations of the results of three experiments performed using clone A3. The inset shows a Northern blot analysis of total RNA extracted from trypanosomes after 2 days of incubation in the absence (−) or presence (+) of tetracycline and probed with [^{32}P]-labeled oligonucleotides used as insertions for the respective stem-loop vectors (top panel); rRNA was stained with ethidium bromide and used as loading control (bottom panel). Two other RNAi clones showed similar growth defects and reductions in TbHMIT mRNA levels upon treatment with tetracycline. (B) *myo*-inositol uptake by *T. brucei* bloodstream forms. After 2 days of incubation in the absence (filled symbols) or presence (open symbols) of tetracycline, RNAi parasites (clone A3) were washed and subsequently incubated with trace amounts of *myo*-[^{3}H]inositol (50 nM final concentration). After the indicated times, parasites were washed, and the amount of radioactivity in the cell pellet was measured. Uptake of *myo*-[^{3}H]inositol at each time point was calculated and plotted as a function of incubation time. Data points represent mean values ± standard deviations of the results of triplicate determinations from three independent experiments. (C) Analysis of *myo*-[^{3}H]inositol-labeled lipids. *T. brucei* bloodstream-form TbHMIT RNAi cells (clone A3) were incubated in the absence or presence of tetracycline for 3 days. During the last 16 h of incubation, parasites (2×10^8 cells) were labeled with 25 μCi of *myo*-[^{3}H]inositol. [^{3}H]-labeled lipids were extracted from parasites incubated in the absence (top panel) or presence (middle panel) of tetracycline to downregulate TbHMIT, separated by one-dimensional TLC using solvent system 1, and visualized by scanning the plate (14). Extracts from cell equivalents were applied. The bottom panel represents extracts from *T. brucei* procyclic forms run on the same TLC plate for comparison, indicating the migration of [^{3}H]inositol phosphorylceramide ([^{3}H]IPC) and [^{3}H]phosphatidylinositol ([^{3}H]PI). The vertical lines indicate the site of sample application (left line) and the migration of the solvent front (right line), respectively. (D) Analysis of [^{3}H]ethanolamine-labeled GPI lipids. Trypanosomes were cultured in the absence (top panel) or presence (middle panel) of tetracycline for 2 days to downregulate TbHMIT and were then labeled during 16 h with [^{3}H]ethanolamine. [^{3}H]GPI lipids were extracted and analyzed by TLC using solvent system 2. The major GPI lipids, designated P2 and P3, were identified based on published R_f values (28) and the migration of [^{3}H]-labeled PP1, i.e., the major GPI precursor lipid in *T. brucei* procyclic forms, run on the same plate (bottom panel). The migration of residual [^{3}H]PE is also indicated. The left and right vertical lines indicate the site of sample application and the migration of the solvent front, respectively.

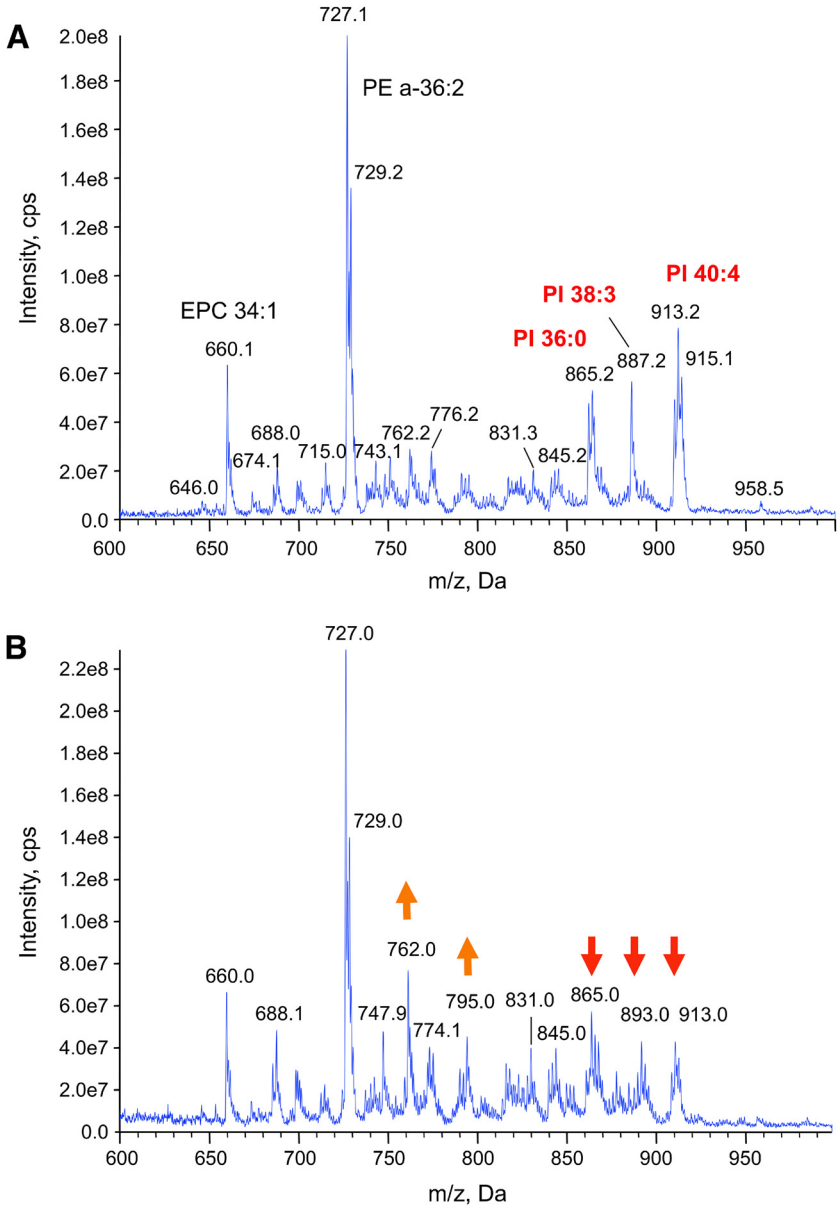

FIG 2 Phospholipid analysis of *T. brucei* bloodstream-form TbHMIT RNAi cells. Lipid extracts from parasites incubated in the absence (A) or presence (B) of tetracycline for 48 h were analyzed by negative-ion ES-MS survey scans (600 to 1,000 *m/z* [mass/charge]). The major phospholipid classes are annotated as follows: PI, phosphatidylinositol; PE, phosphatidylethanolamine; EPC, ethanolamine phosphorylceramide. The arrows in panel B refer to the phospholipid species whose levels increased or decreased after RNAi performed against TbHMIT compared to noninduced cells (A).

phospholipid profile of wild-type parasites (Fig. 2A; see reference 31 for comparison). These include the major plasmalogen (alkenyl acyl) phosphatidylethanolamine (PE) species at 727 *m/z* and PI molecular species at 865, 887, and 913 *m/z*, corresponding to 36:0, 38:3, and 40:4 PI. Upon induction of the RNAi cells for 48 h with tetracycline (Fig. 2B), the intensity of all PI molecular species clearly diminished compared to that seen with uninduced cells, while the plasmalogen PE was still the dominant species (compare Fig. 2A to panel B). To confirm the decrease in the level of the PI molecular species, parent ion scans of 241 *m/z* (the collision-induced inositol-1,2-cyclic phosphate fragment) were recorded (see Fig. S2 in the supplemental material). In extracts of uninduced cells, all major PI species were clearly detected (see Fig. S2A). In contrast, in extracts from parasites after 48 h of tetracycline induction, the intensities of these fragments were drastically decreased (see Fig. S2B). In addition, the amounts of inositol-containing phospholipids were quantified by measuring the *myo*-inositol contents in lipid extracts from control and induced cells and normalizing to cell numbers. The results show that RNAi cells after downregulation of TbHMIT only had 79.5% ± 2.5% *myo*-inositol-containing lipids compared to noninduced cells (100% ± 4% [mean values ± standard deviations of the results from three independent experiments]).

In the induced cells, apart from the reduction in PI species, the intensities of two phospholipid species at 762 and 795 *m/z* had increased (Fig. 2B). These two species were subjected to fragmen-

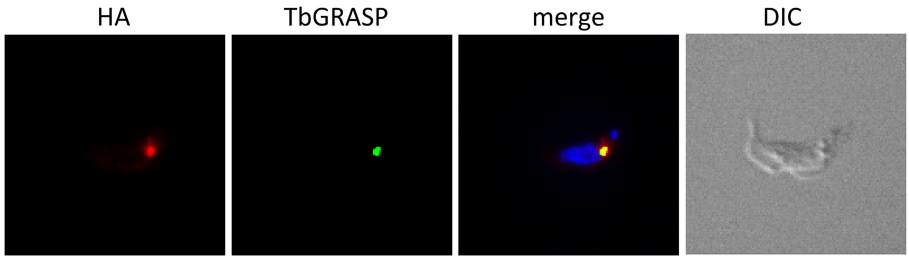

FIG 3 Localization of TbHMIT in *T. brucei* bloodstream forms. Trypanosomes cultured in the presence of tetracycline for 24 h to induce expression of HA-tagged TbHMIT were washed, allowed to settle onto microscope slides, fixed with paraformaldehyde, and permeabilized with Triton X-100. TbHMIT was detected using anti-HA antibody (first panel), whereas the Golgi complex was stained with anti-GRASP antibody (second panel). The third panel shows an overlay of panels A and B, with DNA stained with DAPI. The corresponding differential interference contrast (DIC) micrograph is shown in the fourth panel.

tation (see Fig. S3A and B in the supplemental material, respectively) and identified as PS 34:0 and phosphatidylglycerol (PG) 38:5, respectively. The only other obvious change in the phospholipids was observed in positive-ion mode (see Fig. S4 in the supplemental material), which shows the choline-phosphate-containing species of phosphatidylcholine (PC) and sphingomyelin (SM). The level of the species at 794 *m/z*, representing PC 40:4, was clearly decreased in cells after TbHMIT RNAi compared to that in uninduced cells (compare Fig. S4A with panel B). The cells were obviously trying to compensate for a lack of PI, but the reasons for these specific changes, other than maintenance of the correct membrane fluidity for normal cellular functions, are unknown.

Localization of TbHMIT in *T. brucei* bloodstream forms. Immunofluorescence microscopy revealed that ectopically expressed HA-tagged TbHMIT in *T. brucei* bloodstream forms localized to a distinct intracellular structure located between the nucleus and the kinetoplast (Fig. 3). The signal completely colocalized with TbGRASP (Fig. 3), a marker for the Golgi complex in *T. brucei* (34). These findings are in line with a previous report showing that TbHMIT localizes to the Golgi complex in *T. brucei* procyclic forms (14).

The Golgi complex localization of TbHMIT in *T. brucei* bloodstream forms is noteworthy. It is believed that PI synthesis occurs on the cytosolic side of the ER (10, 35). It should be noted, however, that in several studies in plants (11), yeast (36), protozoa (13), and mammals (12), PI synthase was found to localize not only in the ER but also in close proximity to or in the Golgi complex. As has been demonstrated in *T. brucei* (13, 14), PI synthesis in the ER and PI synthesis in Golgi complex may serve different purposes. PI production in the ER is required for GPI synthesis, while PI produced in the Golgi complex provides bulk PI for membrane formation. Based on the localization of TbHMIT in the Golgi complex, these results suggest that the last step in PI synthesis, i.e., the attachment of *myo*-inositol to cytidine diphosphate-diacylglycerol (CDP-DAG), may occur in the lumen of the Golgi complex. Interestingly, a recent report showed that *T. brucei* CDP-DAG synthase localizes to the ER and the Golgi complex (37), which would be consistent with PI synthesis taking place in the lumen of the ER and the Golgi complex. In addition, results of studies using membrane topology prediction programs TMHMM (38) and Phobius (39) indicate that the active site of *T. brucei* PI synthase is on the luminal side of the ER. On the basis of these observations, we propose the following model for compartmentalization of PI synthesis in *T. brucei* (Fig. 4). In procyclic forms, *myo*-inositol is taken up from the environment via plasma membrane-localized TbHMIT; in bloodstream forms, *myo*-inositol

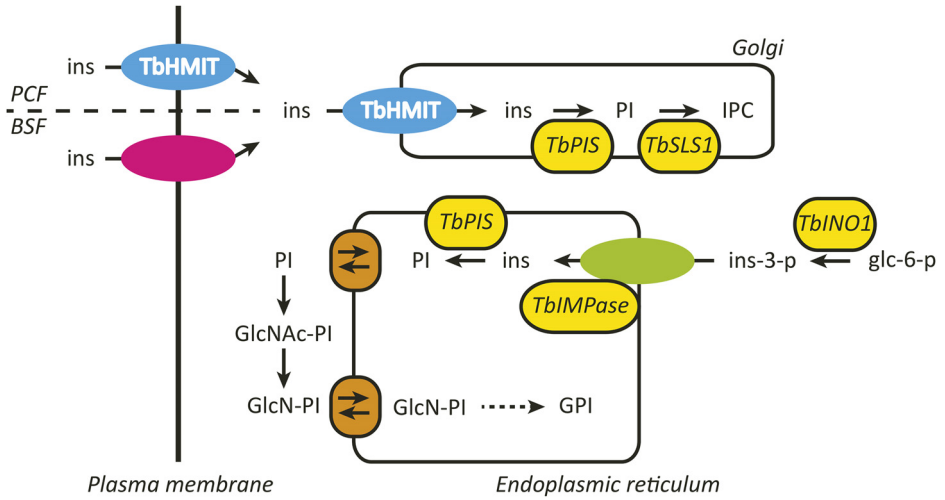

FIG 4 Schematic of compartmentalized *myo*-inositol metabolism in *T. brucei*. For details, see main text. glc-6-P, glucose-6-phosphate; GPI, glycosylphosphatidylinositol; ins, inositol; ins-3-P, inositol-3-phosphate; IPC, inositolphosphoryl ceramide; PI, phosphatidylinositol; TbHMIT, *T. brucei* H^+-coupled *myo*-inositol transporter; GlcNAc-PI, N-acetylglucosaminyl phosphatidylinositol; GlcN-PI, glucosaminyl phosphatidylinositol; TbPIS, *T. brucei* PI synthase; TbSLS1, *T. brucei* sphingolipid synthase 1; TbINO1, *T. brucei* 1-D-*myo*-inositol-3-phosphate synthase; TbIMPase, *T. brucei* inositol monophosphatase.

uptake likely occurs via a different transporter. Cytosolic *myo*-inositol is then transported into the Golgi complex via TbHMIT, where it is used for bulk PI and, subsequently, IPC synthesis. In contrast, *de novo* synthesis of *myo*-inositol starts with the cytosolic conversion of glucose-6-phosphate to inositol-3-phosphate, which in turn is transported into the ER via an unknown transporter. After dephosphorylation, newly synthesized *myo*-inositol is used for PI formation by PI synthase. Subsequently, PI is translocated from the luminal to the cytosolic face of the ER, where it is used to initiate GPI synthesis. Recently, a similar mechanism has also been proposed to occur in the intraerythrocytic stage of the malaria parasite, *Plasmodium falciparum* (40). In addition, it is worth mentioning that the two PI synthase isoforms described in *Arabidopsis thaliana* show different substrate specificities (11), suggesting that two pools of PI may exist and that these may enter alternative routes of metabolism. Furthermore, a Golgi complex localization of PI synthase (11, 12, 36) and HMIT (8) has also been documented in other cells. Thus, we propose that PI formation and metabolism may be similarly compartmentalized in other eukaryotes as well.

Our data using exogenously added *myo*-[^{3}H]inositol showed that, after depletion of TbHMIT by RNAi treatment, uptake of *myo*-[^{3}H]inositol into bloodstream-form parasites still occurred, albeit at a clearly reduced level (Fig. 1B), and yet the formation of [^{3}H]PI was blocked (Fig. 1C). Together with the observed localization of TbHMIT in the Golgi complex, these data suggest that *myo*-[^{3}H]inositol is taken up in *T. brucei* bloodstream forms via a different transporter, located in the plasma membrane, and subsequently remains metabolically inactive because of the lack of the Golgi complex-localized TbHMIT, preventing entry of (cytosolic) *myo*-[^{3}H]inositol into the Golgi complex for [^{3}H]PI production. These results differ slightly from our previous findings in *T. brucei* procyclic forms (14), where treatment with RNAi against TbHMIT blocked not only [^{3}H]PI formation but also *myo*-[^{3}H]inositol uptake into parasites. Interestingly, in procyclic forms, TbHMIT is not only present in the Golgi complex but can also be detected in the plasma membrane, mediating *myo*-[^{3}H]inositol uptake into the cell. We are currently addressing these differences between the bloodstream and procyclic forms with further experiments.

Collectively, these results demonstrate that expression of TbHMIT is essential for normal growth of *T. brucei* bloodstream forms in culture and that it is involved in *myo*-inositol transport into the Golgi complex for PI formation within the lumen of the Golgi complex.

Substrate specificity of TbHMIT. Perfusion of TbHMIT-expressing *Xenopus laevis* oocytes with 200 μM *myo*-inositol resulted in inward currents of 20 ± 1 nA (mean value ± standard deviation, using 13 oocytes from two independent batches). The same concentration of *myo*-inositol did not elicit any currents in water-injected control oocytes. These results are consistent with a previous report (14). To identify other potential substrates, oocytes expressing TbHMIT were exposed to a series of commercially available compounds that are structurally related to *myo*-inositol (Fig. 5). The currents elicited by these compounds (each applied at a concentration of 200 μM) were compared to those obtained with *myo*-inositol (Fig. 6). Interestingly, we found that two quercitol isomers, *epi*- and *vibo*-quercitol, elicited currents comparable to those induced by *myo*-inositol (76% ± 9% and 83% ± 3%, respectively, of the *myo*-inositol current). In contrast, <5% of the current obtained with *myo*-inositol was elicited by another quercitol isomer, *proto*-quercitol (Fig. 6). Quercitols comprise a group of 6-C-containing polyols which, compared to the group of inositol isomers, lack one hydroxyl group (Fig. 5) and, in the case of *proto*-quercitol, contain a C1 epimerization. In addition, low currents (15% to 25% of the *myo*-inositol current) were also obtained with *scyllo*-inositol, *epi*-inositol, 1L-*chiro*-inositol, and phytic acid (*myo*-inositol-1,2,3,4,5,6-hexakisphosphate). In contrast, the currents induced by *muco*-inositol, *allo*-inositol, 1D-*chiro*-inositol, 1L-*epi*-2-inosose (2L-2,3,4,6/5-pentahydroxycyclohexanone), L-quebrachitol (2-O-methyl-L-*chiro*-inositol), D-pinitol (3-O-methyl-D-*chiro*-inositol), N-00601 [(1R,4S)-6-methoxycyclohexane-1,2,3,4,5-pentol], N-50350 [(1R,3S)-6-methoxycyclohexane-1,2,3,4,5-pentol], and D-inositol-3-phosphate represented <5% of the control *myo*-inositol current (Fig. 6).

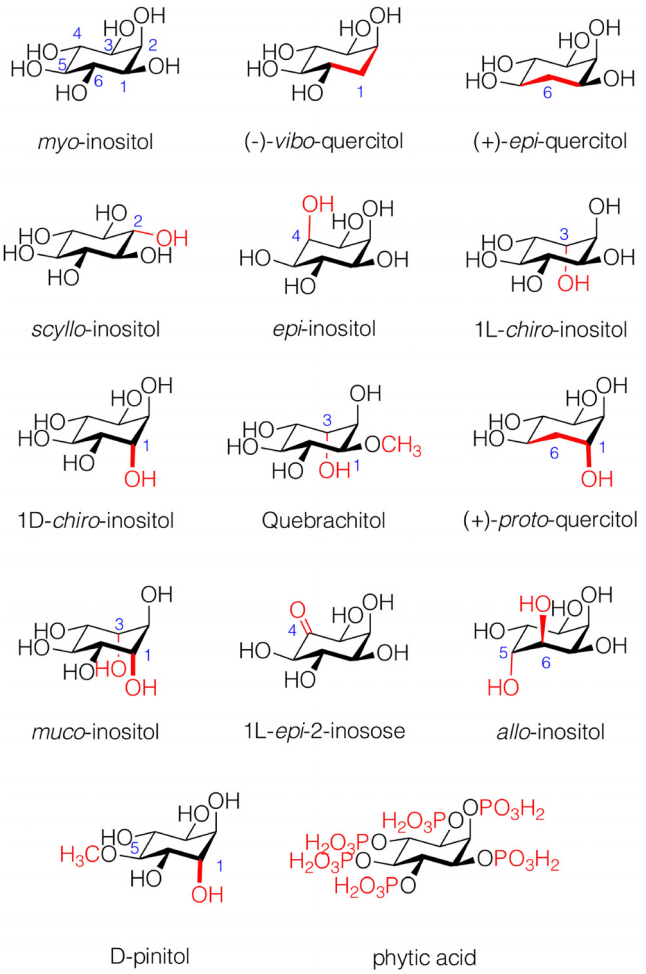

FIG 5 Structures of the various inositols and analogs tested in this study. The numbering refers to the parent *myo*-inositol numbering; the positions and substitutions with a change relative to *myo*-inositol are indicated with the carbon numbers in blue and highlighted in red.

These results, together with our previous findings showing that TbHMIT lacks transport activity for C5 (xylitol) and other C6 (mannitol and sorbitol) polyols and for sugars (glucose and mannose) (14), provide an insight into the selectivity of the transporter in terms of functional groups and stereoselectivity. Among the different analogs tested, deleting a single hydroxyl group at the 1 position [as in (−)-*vibo*-quercitol] or the 6 position [as in (+)-

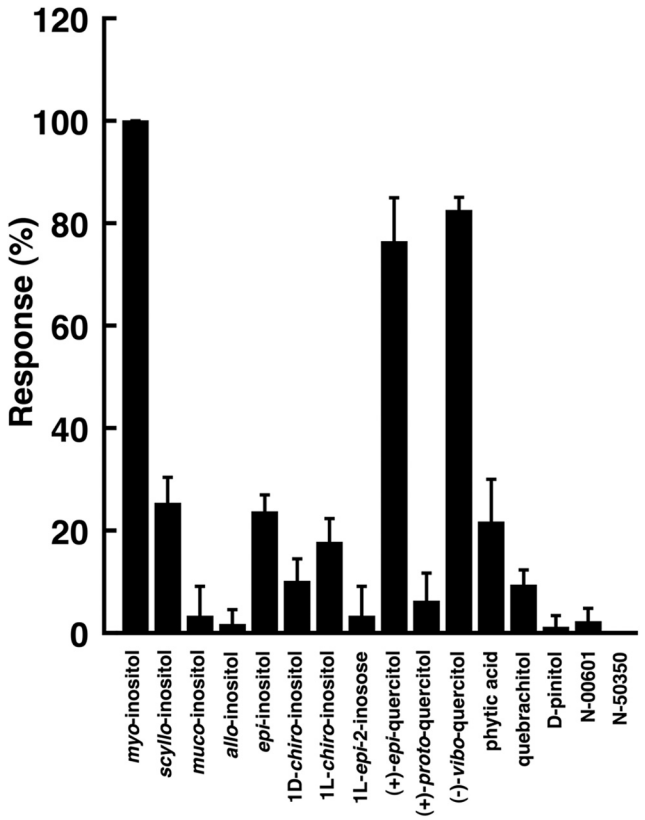

FIG 6 Substrate specificity of TbHMIT. *Xenopus* oocytes expressing TbHMIT were exposed to 200 μM *myo*-inositol and a series of structurally related compounds (all at 200 μM), and the currents were recorded. The bars indicate currents relative to the response elicited by *myo*-inositol (mean values ± standard deviations of the results of at least 3 determinations). N-00601, (1R,4S)-6-methoxycyclohexane-1,2,3,4,5-pentol; N-50350, (1R,3S)-6-methoxycyclohexane-1,2,3,4,5-pentol.

epi-quercitol] induced only a small decrease in current activity. Inversion of stereochemistry at a single hydroxyl group relative to *myo*-inositol was also partly tolerated, leaving 10% to 25% of the current activity seen in *scyllo*-inositol, *epi*-inositol, 1L-*chiro*-inositol, and 1D-*chiro*-inositol. However, a double modification of inositol in terms of inversion of stereochemistry and substitution (deoxy or methyl ether) essentially suppressed all current activity, as seen in quebrachitol, (+)-*proto*-quercitol, *muco*-inositol, *allo*-inositol, and D-pinitol. Note that 1L-*epi*-2-inosose, which features a carbonyl group at position 4 of inositol, showed no transporter activity and that simple carbohydrates such as glucose, galactose, and mannose, which are also structurally related to inositol, were not accepted by the transporter (see reference 14). In addition, all compounds were analyzed for their potential to inhibit TbHMIT-mediated *myo*-inositol transport in *Xenopus* oocytes. Coapplication with *myo*-inositol showed that none of compounds affected the *myo*-inositol-elicited currents, demonstrating that they did not act as inhibitors of TbHMIT at the concentrations tested. Finally, to establish the apparent affinities of TbHMIT for transport of *epi*- and *vibo*-quercitol, *Xenopus* oocytes were exposed to increasing concentrations of the compounds and currents were recorded. The results showed that the 50% effective concentrations (EC_{50}s) for *epi*- and *vibo*-quercitol (121 μM and 104 μM, respectively [mean values from 2 independent experiments]) were in the same range as that for *myo*-inositol (61 μM; see reference 14).

Together, these data show that TbHMIT is remarkably selective for *myo*-inositol. It tolerates a single modification on the inositol ring only, such as the removal of a hydroxyl group at position 1 or position 6 or the inversion of stereochemistry at a single hydroxyl group relative to *myo*-inositol, but no additional modifications. Interestingly, TbHMIT (14) and its orthologs from *T. cruzi* (20) and *Leishmania* parasites (18, 41) show no transport activity for monosaccharides. This is in marked contrast to all other members of the GLUT/SLC2A family, including the intracellularly located members of subclass III, which transport many different monosaccharides (1, 5, 6). In addition, HMIT's transport specificity is also different from that of the SMITs, which transport both *myo*-inositol and monosaccharides (2, 3).

ACKNOWLEDGMENTS

This work was supported by Swiss National Science Foundation Sinergia grant CRSII3_141913 to P.B. and E.S., Wellcome Trust grant 093228 to T.K.S., and the NCCR TransCure support to J.-L.R.

D-*myo*-Inositol-3-phosphate was prepared by Lloyd Sayer (University of St Andrews). We thank J. Jelk for technical help with the GPI labeling experiments. P.B. thanks M. Bütikofer for support, A. K. Menon for discussions, and I. Dragons for stimulation.

REFERENCES

1. **Wright EM, Loo DD, Hirayama BA.** 2011. Biology of human sodium glucose transporters. Physiol Rev **91:**733–794. http://dx.doi.org/10.1152/physrev.00055.2009.
2. **Hager K, Hazama A, Kwon HM, Loo DD, Handler JS, Wright EM.** 1995. Kinetics and specificity of the renal Na^+/*myo*-inositol cotransporter expressed in *Xenopus* oocytes. J Membr Biol **143:**103–113.
3. **Coady MJ, Wallendorff B, Gagnon DG, Lapointe JY.** 2002. Identification of a novel Na^+/*myo*-inositol cotransporter. J Biol Chem **277:**35219–35224. http://dx.doi.org/10.1074/jbc.M204321200.
4. **Joost HG, Bell GI, Best JD, Birnbaum MJ, Charron MJ, Chen YT, Doege H, James DE, Lodish HF, Moley KH, Moley JF, Mueckler M, Rogers S, Schurmann A, Seino S, Thorens B.** 2002. Nomenclature of the GLUT/SLC2A family of sugar/polyol transport facilitators. Am J Physiol Endocrinol Metab **282:**E974–E976. http://dx.doi.org/10.1152/ajpendo.00407.2001.
5. **Augustin R.** 2010. The protein family of glucose transport facilitators: it's not only about glucose after all. IUBMB Life **62:**315–333. http://dx.doi.org/10.1002/iub.315.
6. **Cura AJ, Carruthers A.** 2012. Role of monosaccharide transport proteins in carbohydrate assimilation, distribution, metabolism, and homeostasis. Compr Physiol **2:**863–914. http://dx.doi.org/10.1002/cphy.c110024.
7. **Flessner LB, Moley KH.** 2009. Similar [DE]XXXL[LI] motifs differentially target GLUT8 and GLUT12 in Chinese hamster ovary cells. Traffic **10:**324–333. http://dx.doi.org/10.1111/j.1600-0854.2008.00866.x.
8. **Di Daniel E, Mok MH, Mead E, Mutinelli C, Zambello E, Caberlotto LL, Pell TJ, Langmead CJ, Shah AJ, Duddy G, Kew JN, Maycox PR.** 2009. Evaluation of expression and function of the H^+/*myo*-inositol transporter HMIT. BMC Cell Biol **10:**54. http://dx.doi.org/10.1186/1471-2121-10-54.
9. **Michell RH.** 2013. Inositol lipids: from an archaeal origin to phosphatidylinositol 3,5-bisphosphate faults in human disease. FEBS J **280:**6281–6294. http://dx.doi.org/10.1111/febs.12452.
10. **Fischl AS, Homann MJ, Poole MA, Carman GM.** 1986. Phosphatidylinositol synthase from *Saccharomyces cerevisiae*. Reconstitution, characterization, and regulation of activity. J Biol Chem **261:**3178–3183.
11. **Löfke C, Ischebeck T, König S, Freitag S, Heilmann I.** 2008. Alternative metabolic fates of phosphatidylinositol produced by phosphatidylinositol synthase isoforms in *Arabidopsis thaliana*. Biochem J **413:**115–124. http://dx.doi.org/10.1042/BJ20071371.
12. **Batenburg JJ, Klazinga W, van Golde LM.** 1985. Regulation and location of phosphatidylglycerol and phosphatidylinositol synthesis in type II cells isolated from fetal rat lung. Biochim Biophys Acta **833:**17–24. http://dx.doi.org/10.1016/0005-2760(85)90248-6.
13. **Martin KL, Smith TK.** 2006. Phosphatidylinositol synthesis is essential in

bloodstream form *Trypanosoma brucei*. Biochem J **396:**287–295. http://dx.doi.org/10.1042/BJ20051825.
14. **Gonzalez-Salgado A, Steinmann ME, Greganova E, Rauch M, Mäser P, Sigel E, Bütikofer P.** 2012. *myo*-Inositol uptake is essential for bulk inositol phospholipid but not glycosylphosphatidylinositol synthesis in *Trypanosoma brucei*. J Biol Chem **287:**13313–13323. http://dx.doi.org/10.1074/jbc.M112.344812.
15. **Martin KL, Smith TK.** 2006. The glycosylphosphatidylinositol (GPI) biosynthetic pathway of bloodstream-form *Trypanosoma brucei* is dependent on the *de novo* synthesis of inositol. Mol Microbiol **61:**89–105. http://dx.doi.org/10.1111/j.1365-2958.2006.05216.x.
16. **Drew ME, Langford CK, Klamo EM, Russell DG, Kavanaugh MP, Landfear SM.** 1995. Functional expression of a *myo*-inositol/H^+ symporter from *Leishmania donovani*. Mol Cell Biol **15:**5508–5515.
17. **Klamo EM, Drew ME, Landfear SM, Kavanaugh MP.** 1996. Kinetics and stoichiometry of a proton/*myo*-inositol cotransporter. J Biol Chem **271:**14937–14943. http://dx.doi.org/10.1074/jbc.271.25.14937.
18. **Seyfang A, Landfear SM.** 2000. Four conserved cytoplasmic sequence motifs are important for transport function of the *Leishmania* inositol/H^+ symporter. J Biol Chem **275:**5687–5693. http://dx.doi.org/10.1074/jbc.275.8.5687.
19. **Mongan TP, Ganapasam S, Hobbs SB, Seyfang A.** 2004. Substrate specificity of the *Leishmania donovani myo*-inositol transporter: critical role of inositol C-2, C-3 and C-5 hydroxyl groups. Mol Biochem Parasitol **135:**133–141. http://dx.doi.org/10.1016/j.molbiopara.2004.01.015.
20. **Einicker-Lamas M, Almeida AC, Todorov AG, de Castro SL, Caruso-Neves C, Oliveira MM.** 2000. Characterization of the *myo*-inositol transport system in *Trypanosoma cruzi*. Eur J Biochem **267:**2533–2537. http://dx.doi.org/10.1046/j.1432-1327.2000.01302.x.
21. **Einicker-Lamas M, Nascimento MT, Masuda CA, Oliveira MM, Caruso-Neves C.** 2007. *Trypanosoma cruzi* epimastigotes: regulation of *myo*-inositol transport by effectors of protein kinases A and C. Exp Parasitol **117:**171–177. http://dx.doi.org/10.1016/j.exppara.2007.04.011.
22. **Wirtz E, Leal S, Ochatt C, Cross GM.** 1999. A tightly regulated inducible expression system for conditional gene knock-outs and dominant-negative genetics in *Trypanosoma brucei*. Mol Biochem Parasitol **99:**89–101. http://dx.doi.org/10.1016/S0166-6851(99)00002-X.
23. **Shlomai J.** 2004. The structure and replication of kinetoplast DNA. Curr Mol Med **4:**623–647. http://dx.doi.org/10.2174/1566524043360096.
24. **Brun R, Schönenberger M.** 1979. Cultivation and *in vitro* cloning or procyclic culture forms of *Trypanosoma brucei* in a semi-defined medium. Acta Trop **36:**289–292.
25. **Serricchio M, Bütikofer P.** 2013. Phosphatidylglycerophosphate synthase associates with a mitochondrial inner membrane complex and is essential for growth of *Trypanosoma brucei*. Mol Microbiol **87:**569–579. http://dx.doi.org/10.1111/mmi.12116.
26. **Schumann Burkard G, Jutzi P, Roditi I.** 2011. Genome-wide RNAi screens in bloodstream form trypanosomes identify drug transporters. Mol Biochem Parasitol **175:**91–94. http://dx.doi.org/10.1016/j.molbiopara.2010.09.002.
27. **Bütikofer P, Ruepp S, Boschung M, Roditi I.** 1997. 'GPEET' procyclin is the major surface protein of procyclic culture forms of *Trypanosoma brucei brucei* strain 427. Biochem J **326:**415–423.
28. **Mayor S, Menon AK, Cross GA.** 1990. Glycolipid precursors for the membrane anchor of *Trypanosoma brucei* variant surface glycoproteins. II. Lipid structures of phosphatidylinositol-specific phospholipase C sensitive and resistant glycolipids. J Biol Chem **265:**6174–6181.
29. **Bütikofer P, Lin ZW, Kuypers FA, Scott MD, Xu CM, Wagner GM, Chiu DT, Lubin B.** 1989. Chlorpromazine inhibits vesiculation, alters phosphoinositide turnover and changes deformability of ATP-depleted RBCs. Blood **73:**1699–1704.
30. **Bligh EG, Dyer WJ.** 1959. A rapid method of total lipid extraction and purification. Can J Biochem Physiol **37:**911–917. http://dx.doi.org/10.1139/o59-099.
31. **Richmond GS, Gibellini F, Young SA, Major L, Denton H, Lilley A, Smith TK.** 2010. Lipidomic analysis of bloodstream and procyclic form *Trypanosoma brucei*. Parasitology **137:**1357–1392. http://dx.doi.org/10.1017/S0031182010000715.
32. **Ferguson MAJ.** 1993. GPI membrane anchors: isolation and analysis, p 349–383. *In* Fukuda M, Kobata A (ed), Glycobiology: a practical approach, vol 125. IRL Press at Oxford University Press, Bethesda, MD.
33. **Sutterwala SS, Hsu FF, Sevova ES, Schwartz KJ, Zhang K, Key P, Turk J, Beverley SM, Bangs JD.** 2008. Developmentally regulated sphingolipid synthesis in African trypanosomes. Mol Microbiol **70:**281–296. http://dx.doi.org/10.1111/j.1365-2958.2008.06393.x.
34. **He CY, Ho HH, Malsam J, Chalouni C, West CM, Ullu E, Toomre D, Warren G.** 2004. Golgi duplication in *Trypanosoma brucei*. J Cell Biol **165:**313–321. http://dx.doi.org/10.1083/jcb.200311076.
35. **Nikawa J, Yamashita S.** 1997. Phosphatidylinositol synthase from yeast. Biochim Biophys Acta **1348:**173–178. http://dx.doi.org/10.1016/S0005-2760(97)00103-3.
36. **Leber A, Hrastnik C, Daum G.** 1995. Phospholipid-synthesizing enzymes in Golgi membranes of the yeast, *Saccharomyces cerevisiae*. FEBS Lett **377:**271–274. http://dx.doi.org/10.1016/0014-5793(95)01361-X.
37. **Lilley AC, Major L, Young S, Stark MJ, Smith TK.** 2014. The essential roles of cytidine diphosphate-diacylglycerol synthase in bloodstream form *Trypanosoma brucei*. Mol Microbiol **92:**453–470. http://dx.doi.org/10.1111/mmi.12553.
38. **Krogh A, Larsson B, von Heijne G, Sonnhammer EL.** 2001. Predicting transmembrane protein topology with a hidden Markov model: application to complete genomes. J Mol Biol **305:**567–580. http://dx.doi.org/10.1006/jmbi.2000.4315.
39. **Käll L, Krogh A, Sonnhammer EL.** 2007. Advantages of combined transmembrane topology and signal peptide prediction–the Phobius web server. Nucleic Acids Res **35:**W429–W432. http://dx.doi.org/10.1093/nar/gkm256.
40. **Macrae JI, Lopaticki S, Maier AG, Rupasinghe T, Nahid A, Cowman AF, McConville MJ.** 2014. *Plasmodium falciparum* is dependent on *de novo myo*-inositol biosynthesis for assembly of GPI glycolipids and infectivity. Mol Microbiol **91:**762–776. http://dx.doi.org/10.1111/mmi.12496.
41. **Seyfang A, Kavanaugh MP, Landfear SM.** 1997. Aspartate 19 and glutamate 121 are critical for transport function of the *myo*-inositol/H^+ symporter from *Leishmania donovani*. J Biol Chem **272:**24210–24215. http://dx.doi.org/10.1074/jbc.272.39.24210.